



# Recent Developments on Colloidal Deposits Obtained by Evaporation of Sessile Droplets on a Solid Surface

Nagesh D. Patil<sup>1\*</sup> and Rajneesh Bhardwaj<sup>2\*</sup>

**Abstract** | Understanding flow patterns and coupled transport phenomena during evaporation of droplets loaded with colloidal particles is central to design technical applications such as organizing proteins/DNA on a solid surface. We review recent reports on evaporating sessile droplets of colloidal suspensions on a solid surface. Starting from the classical mechanism of formation of a ring-like deposit, we discuss the influence of several problem parameters. Notably, thermal or solutal Marangoni effect, particle size, particle concentration, particle shape, substrate wettability, pH of the suspension, etc. have been found important in controlling the deposition pattern. The deposit pattern complexity and shape have been attributed to the underlying coupled transport phenomena during the evaporation. We discuss important regime maps reported for different types of deposits, which allow us to classify the deposits and coupled physics. We also present studies that have demonstrated particles sorting in an evaporating bidispersed colloidal suspension on a solid surface. Finally, some remarks for the future research opportunities in this arena are presented.

**Keywords:** *Sessile droplet evaporation, Colloidal deposits, Marangoni convection, Coffee-ring effect*

## 1 Introduction

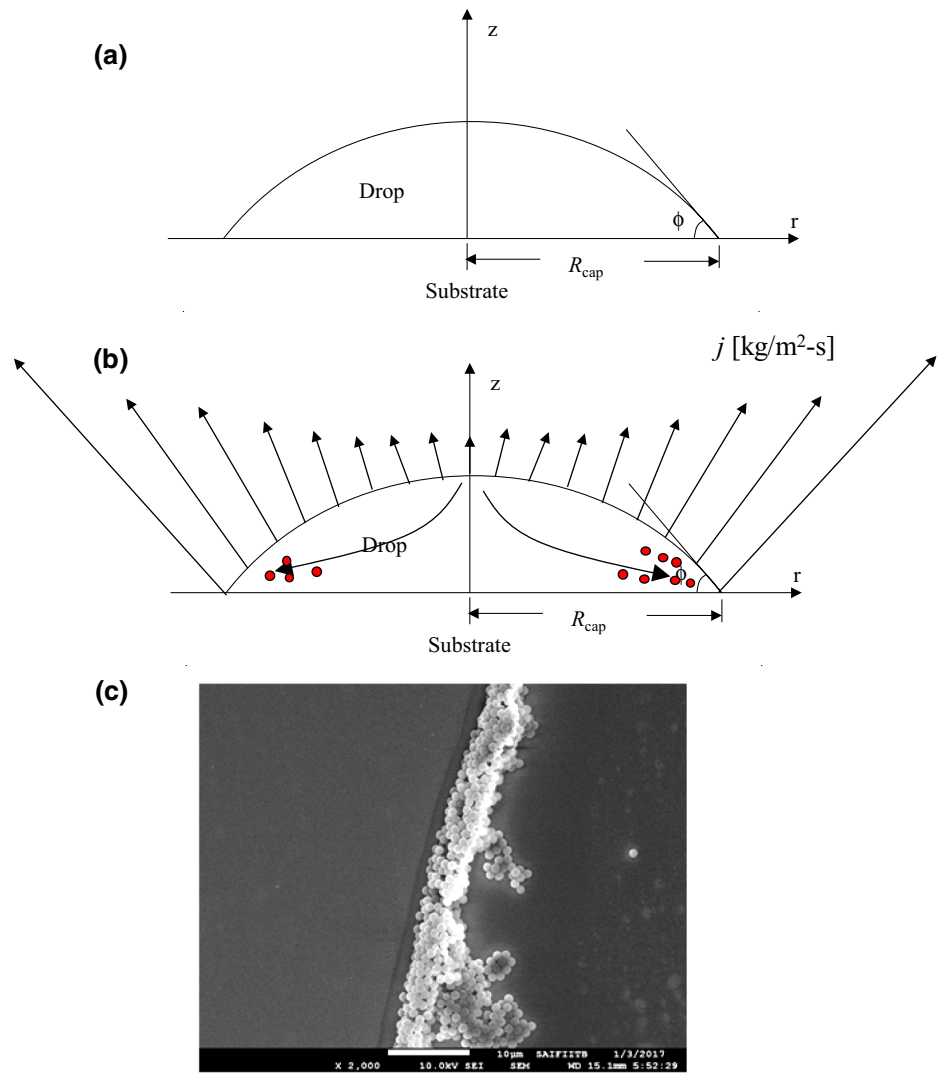
The evaporation of a droplet containing colloidal particles on a solid surface is a topic of interest in the research community for the last two decades<sup>1</sup>. Several extensive studies have been performed because of potential applications in inkjet printing<sup>2</sup>, surface coating<sup>3</sup>, biochemistry analysis<sup>4</sup>, biosensor and diagnostics<sup>5</sup>, forensic<sup>6</sup>, etc. As investigated by Deegan et al.<sup>7</sup>, the evaporation mass flux along the liquid–gas interface is non-uniform and is the largest near the contact line (schematically shown in Fig. 1b), which creates radially outward fluid flow inside the droplet; the contact line of the droplet is pinned due to the microscopic surface roughness. Here, the evaporation takes place by diffusion of liquid vapor from a spherical cap-like sessile droplet on the

surface. Thus, an evaporating droplet dispersed with colloidal particles results in a ring-like particle deposit, due to the advection of the particles by the outward fluid flow<sup>7</sup>, as shown in Fig. 1c, showing a zoomed-in SEM image of the ring. The physics of the droplet evaporation is coupled at disparate time and length scales. For instance, the deposition of the droplet involves impact of the droplet at a much faster timescale, followed by a much slower scale for the evaporation. For instance, a nanoliter droplet on a heated fused silica substrate takes around 10 ms for impact and 4 s for complete evaporation<sup>8</sup> (Fig. 2). Table 1 summarizes all possible transport phenomena and Fig. 3 shows these processes using a schematic. A general research question to answer is how flow field in the droplet and other transport

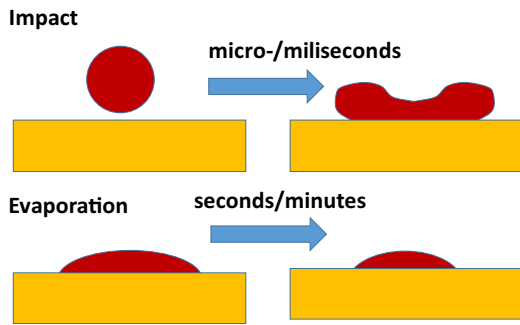
<sup>1</sup> Department of Mechanical Engineering, University of British Columbia, Vancouver V6T 1Z4, BC, Canada.

<sup>2</sup> Department of Mechanical Engineering, Indian Institute of Technology Bombay, Mumbai 400076, India.

\*nagesh.patil@ubc.ca  
rajneesh.bhardwaj@iitb.ac.in



**Figure 1:** **a** Schematic of the evaporation of a sessile droplet on a solid surface. **b** Advection of colloidal particles (shown as red circles) during the evaporation. The evaporative flux on the liquid–gas interface is shown by vectors, exhibiting the non-uniformity of the flux on the liquid–gas interface. **c** SEM image of a typical ring obtained after the drying of an water droplet loaded with 1.1 micrometers polystyrene particles (Reprinted from Ref.<sup>30</sup> with permission). Copyright (2018) American Chemical Society.

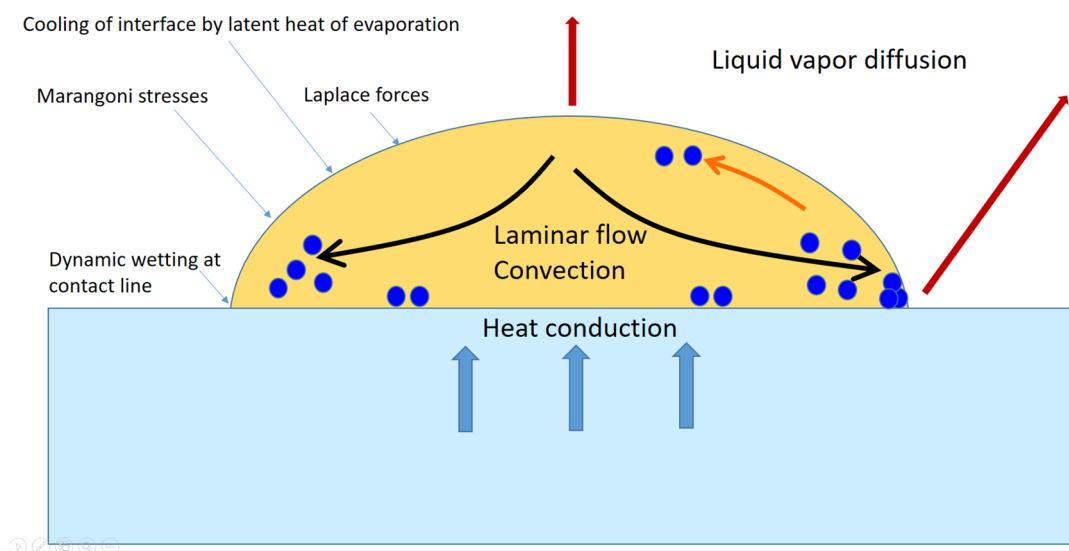


**Figure 2:** Differences in the timescale of an impacting droplet versus an evaporating micro-liter or millimeter size water droplet. The evaporation scale is much slower owing to slow diffusion of liquid vapor in the ambient.

phenomena influence the colloidal deposit formed after the evaporation. Various deposit patterns can be observed, as reported in recent reviews by Larson<sup>9</sup>, Sefiane<sup>10</sup> and Parsa et al.<sup>11</sup>. A most common example of deposit pattern is the drying of a droplet with particles, such as a coffee spill, which forms a ring-like pattern on the surface. This is called the “coffee-ring” effect, a term coined by Deegan et al.<sup>7</sup>. In the following, we review the recent key studies, which investigated the role and effect of important problem parameters in the context of the formation of colloidal deposits using the evaporation of droplets.

**Table 1:** Summary of the possible transport phenomena for an evaporating droplet laden with colloidal particles on a heated surface.

Fluid dynamics	Incompressible and laminar fluid flow Viscosity variation due to temperature change Laplace forces on the liquid–gas boundary Motion of the wetting line during advancing or receding phase Marangoni stresses along the liquid–gas interface
Heat transfer	Convection inside the drop and conduction in the substrate Imperfect thermal contact between the droplet and the substrate
Mass transfer	Diffusion of liquid vapor in the ambient of the droplet Evaporative-driven flow inside the droplet Cooling of the drop at the liquid–gas interface by latent heat of evaporation
Particle transport	Advection–diffusion of the particles inside the droplet Interactions of free surface with growing peripheral deposit of the particles Attractive or repulsive forces between the particles and the substrate Inter-particle forces

**Figure 3:** Schematic of an evaporation of a sessile droplet loaded with colloidal particles on a solid surface. Several coupled transport phenomena are shown in the schematic.

## 2 Role of Contact Line Depinning

Droplet evaporation involves two modes, the constant contact radius (CCR) mode, where the contact radius stays constant with the contact angle decreasing, and the constant contact angle (CCA) mode, where the contact angle remains constant with the contact radius decreasing<sup>12</sup>, i.e., depinning of the contact line. The CCR mode is more likely to happen on hydrophilic substrates, while the CCA mode is more usual on hydrophobic substrates<sup>11</sup>. The combination of the two modes generates various particle deposition patterns, as shown in Fig. 4. If the evaporation occurs in CCR mode, then a ring-like deposit forms<sup>13</sup> and if it occurs with depinning of contact line, i.e., CCA mode, then an inner deposit forms<sup>14</sup>. Moreover, if

the evaporation occurs with stick–slip motion of the contact line (combination of CCR and CCA), then multiple-ring deposit forms<sup>15</sup>.

Sangani et al.<sup>16</sup> studied the droplet evaporation containing colloidal particles for a wide range of particle diameters ( $d_p = 1\text{--}70\ \mu\text{m}$ ). They calculated the surface tension force acting on the particle near the contact line and gave a criterion for the contact line pinning. Further, Jung et al.<sup>17</sup> and Wong et al.<sup>18</sup> explained that the deposit patterns depend on the evaporation mechanism of the droplet on the surface. During evaporation, the particles inside the droplet experience several forces, namely, surface tension (or capillary) force, drag force, friction force, and adhesion forces due to the van der Waals force and

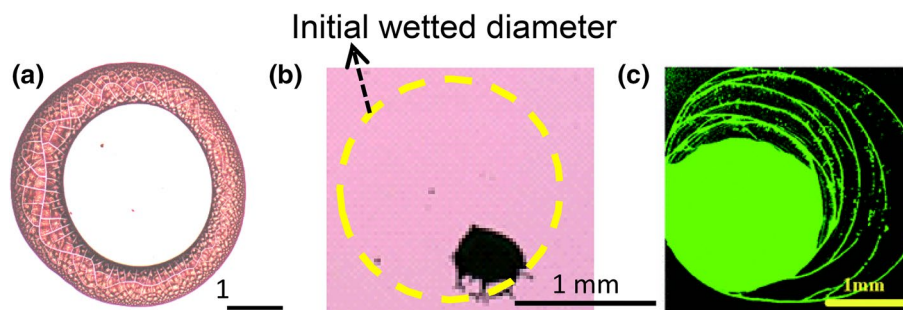


**Figure 4:** Various particle deposit patterns due to different modes of evaporation. **a** Ring-like pattern (reprinted with permission from Ref. <sup>13</sup>, Copyright (2004) American Chemical Society), **b** inner deposit (reprinted with permission from Ref. <sup>14</sup>, Copyright (2016) American Chemical Society), **c** multiple ring patterns (reprinted with permission from Ref. <sup>15</sup>, Copyright (2008) American Physical Society).

electrostatic interaction forces between particles and substrate, as well as among the particles themselves inside the fluid. The particle deposition near the contact line is the result of the competition between these forces acting on each of the particles near the contact line. During the evaporation, as the inward surface tension force overcomes all other forces, the depinning of the contact line occurs; otherwise not<sup>16,19</sup>. There are several studies that shows the contact line pinning and coffee-ring formation<sup>10</sup>. But, from the application point of view, researchers have investigated several ways to change or control the coffee-ring effect, summarized recently by Parsa et al.<sup>11</sup>.

### 3 Effect of Substrate Heating

Recently, various research groups have investigated that the coffee-ring effect can be suppressed by varying the surface tension gradients of the liquid–gas interface, though the droplet was evaporating in the CCR mode. It can be caused by varying substrate temperatures<sup>20,21</sup> which induced thermal Marangoni stresses at the liquid–gas interface. This generates a convective flow near the liquid–gas interface from the lower surface tension region (droplet contact point) to the higher surface tension region (droplet apex point), called thermal Marangoni flow. The Marangoni circulation reverses the outward capillary flow of particles and changes the particle deposition from the ring to the droplet center region<sup>22</sup>. Note that a thermal Marangoni flow also exists due to non-uniform cooling of the interface by latent heat of evaporation. Hu and Larson<sup>23</sup> and Bhardwaj et al.<sup>24</sup> reported that such a Marangoni flow can suppress the coffee-ring effect.

Recently, few studies which used substrate heating have been carried out. For example, Li et al.<sup>20</sup> varied glass ( $\theta_{eq}=24^{\circ}$ – $30^{\circ}$ ) surface

temperature from  $T_s=30$ – $80$  °C and obtained various deposit patterns as shown in Fig. 5. They studied the evaporation of  $2.5$   $\mu\text{L}$  water droplets containing  $0.25\%$  (v/v),  $100$  nm polystyrene particles. The deposit pattern changes from coffee ring to a “coffee eye”—thin ring with an inner deposit with increase in substrate temperature. In the figure, at heated substrate temperature, the inner deposit increases due to higher Marangoni recirculation inside the droplet, which brings more particles toward the droplet center. Further, Parsa et al.<sup>21</sup> varied the surface temperature from  $T_s=25$ – $99$  °C and obtained a uniform deposit pattern to a dual-ring pattern transformation on a smooth silicon surface ( $\theta_{eq}=30^{\circ}$ – $40^{\circ}$ ), as shown in Fig. 6. They used  $0.05\%$  (w/w) copper oxide nanoparticles. They demonstrated that uniform particle deposit changes to dual-ring pattern and the size of the secondary ring changes with increase in the substrate temperature. At the highest substrate temperature, a stick–slip motion was found which gave rise to multi-ring patterns. Similarly, Zhong and Duan<sup>25</sup> studied the evaporation of droplets containing graphite nanopowders of  $d_p=2$ – $3$  nm particles with  $c=0.05\%$  (v/v). The substrate temperature was varied from  $T_s=10$ – $50$  °C. They also found uniform deposition of particle changes to dual-ring (outer thin ring and inner thick ring) patterns with increase in substrate temperature, as shown in Fig. 7. Further, Patil et al.<sup>14</sup> studied the effect of substrate heating ( $T_s=27$ – $90$  °C) on hydrophilic glass ( $\theta_{eq}=34^{\circ}$ – $38^{\circ}$ ) and hydrophobic silicon ( $\theta_{eq}=94^{\circ}$ – $97^{\circ}$ ). They considered the evaporation of droplets containing  $d_p=0.46$   $\mu\text{m}$  polystyrene particles with different particle concentrations,  $c=0.05$ ,  $0.1$  and  $1.0\%$  (v/v), and proposed a regime map showing three deposit patterns, namely, ring, thin ring with inner

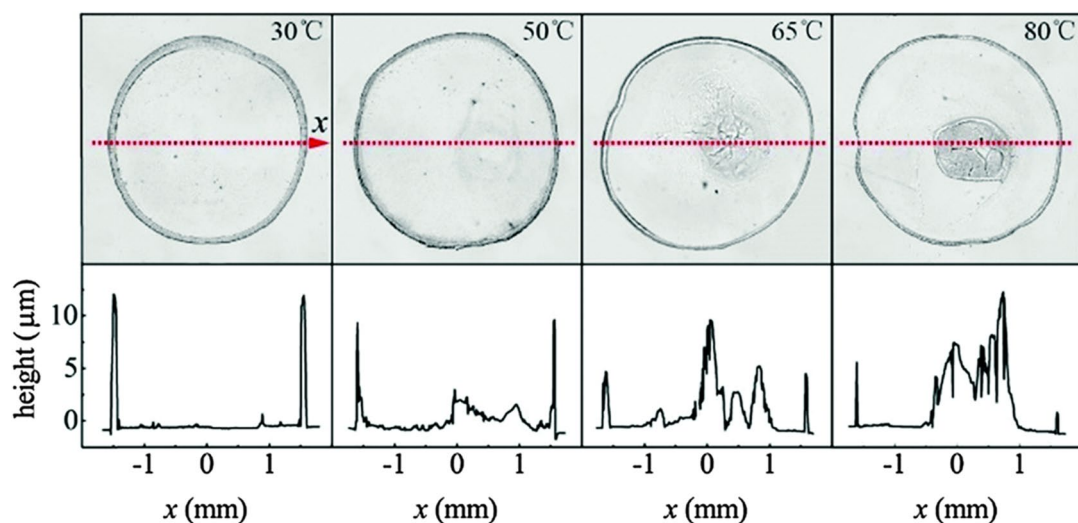


**Figure 5:** Dried deposit patterns obtained at different glass substrate temperature. Second row shows ring width and height at the corresponding cross sections measured by interferometry along the red lines. Inner deposit increases with increase in the substrate temperature, and thus the ring becomes thinner. Reprinted with permission from Ref.<sup>40</sup>. Copyright (2015) Royal Society Of Chemistry.

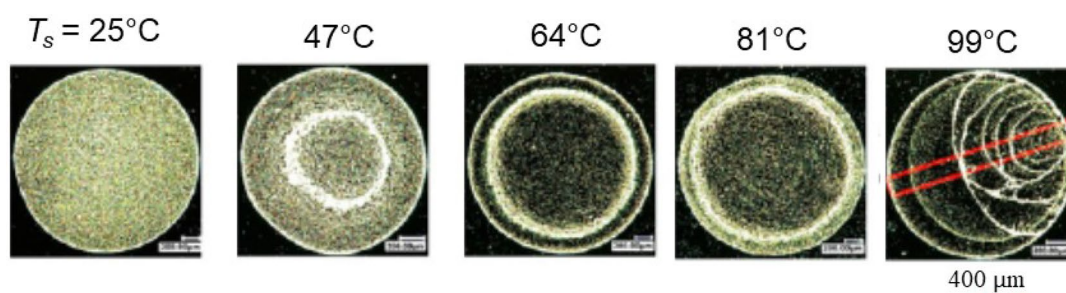


**Figure 6:** Final deposit patterns obtained on silicon at different surface temperatures. Deposit patterns transform from uniform deposits to dual-ring- and multi-ring-like deposits. Reprinted with permission from Ref.<sup>41</sup>, Copyright (2015) American Chemical Society.

deposit, and inner deposit, as shown in Fig. 8. At ambient, as expected a ring and an inner deposit formed on glass and silicon, respectively. At higher substrate temperature, a thin ring with inner deposit formed on both substrates. In all of the above studies, the thinning of the ring and formation of either inner deposit or the dual ring were attributed to the Marangoni convection inside the droplet that transports the particles from the contact line region to the inner region of the droplet.

#### 4 Effect of Particle Size

The particle size can also influence the deposit patterns. In this regard, recently various studies were performed on the evaporation of a droplet containing colloidal suspensions of

different particle diameters. Perelaer et al.<sup>26</sup> used colloidal suspensions of silica particles of diameter  $d_p = 0.33, 1, 3$  and  $5 \mu\text{m}$  ( $c = 1\%$  w/w) on different glass substrates ( $\theta_{\text{eq}} = 5^\circ - 130^\circ$ ). They found that for smaller particle sizes, ring-like patterns are formed on lesser contact angle substrates, and for larger particle sizes inner deposit or uniform deposit patterns are formed on all tested substrates. A similar type of particle deposit pattern behavior was recorded by Biswas et al.<sup>27</sup> for polystyrene particles of diameter  $d_p = 0.02, 0.2$  and  $1.1 \mu\text{m}$  ( $c = 0.05\%$  w/w) on different glass substrates. They showed that the particle size significantly affected the deposit patterns and reported that the particle deposited at the contact line as per its geometric sizes. Weon and Je<sup>19</sup> studied the effect of two particle sizes,  $d_p = 0.1$  and

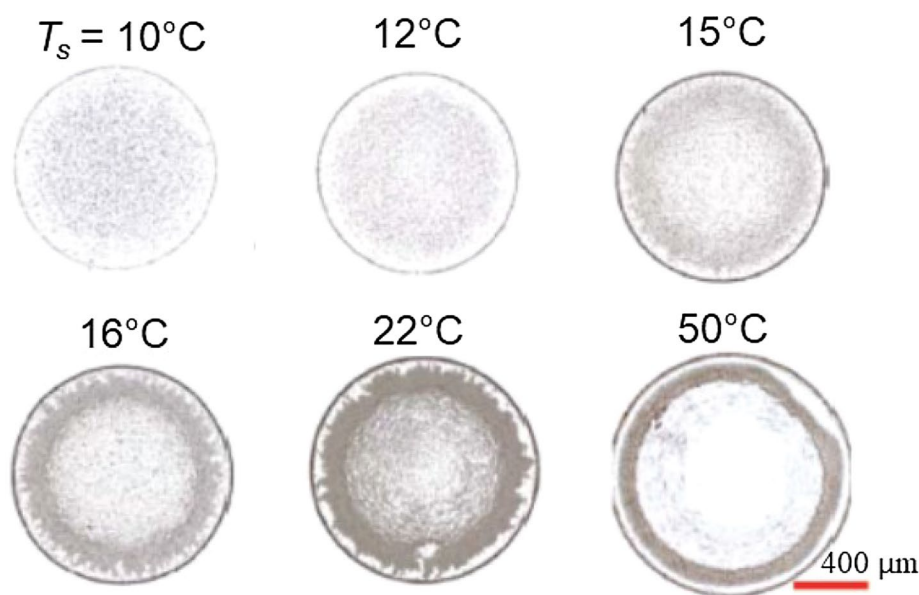


**Figure 7:** Deposit patterns obtained on silicon wafer as a function of substrate temperature. Deposit patterns transform from uniform deposits to dual-ring deposits. Reprinted with permission from Ref.<sup>25</sup>. Copyright (2016) Royal Society Of Chemistry

1.0  $\mu\text{m}$  ( $c=1\%$  w/w), on glass ( $\theta_{\text{eq}}=15^\circ$ ). They explained that smaller size particles were easily pinned at the contact line, as they were larger in number and could get closely packed next to each other during evaporation, in comparison to larger size particles which were lesser in number and loosely deposited next to each other at the contact line. As a result, after complete dry-out smaller size particles form a ring and larger size particles do not form a ring-like deposit.

Recently, Ryu et al.<sup>28</sup> reported the deposit patterns for particle sizes from 100 nm to 10  $\mu\text{m}$  diameters, as shown in Fig. 9, and showed that the ring-like deposit is formed for smaller colloids while uniform deposit pattern is formed for larger colloids. Further, they also studied the effect of polyethylene oxide (PEO) polymer concentration in the same solution and even for larger colloids obtained ring-like deposits. Malla et al.<sup>29</sup> observed the ring-like deposits for all particle sizes ( $d_p=0.1\text{--}3\ \mu\text{m}$ ) on hydrophilic glass. However they reported that in the formed ring, the particles' morphologies change with the particle size and the particle concentration ( $c=0.001\text{--}1\%$ , v/v). They proposed a regime map of particle deposit morphologies showing discontinuous monolayer ring, continuous monolayer ring, and multiple layers ring.

The effect of particle size coupled with substrate heating has also been reported. Patil et al.<sup>30</sup> investigated the combined effect of substrate

temperature ( $T_s=27\text{--}90\ ^\circ\text{C}$ ) and particle size ( $d_p=0.1\text{--}3\ \mu\text{m}$ ) on the deposit patterns as shown in Fig. 10. They showed that on non-heated silicon substrate ( $\theta_{\text{eq}}=85^\circ$ ), for smaller size particles inner deposit forms and for larger size particles a ring-like structure forms. While on heated silicon substrate, for all tested particle sizes, a thin ring with inner deposit patterns form. They showed that due to the combined effect of substrate heating and colloidal suspensions, the contact line pins on higher contact angle substrate ( $\theta_{\text{eq}}=85^\circ$ ) and it changes the deposit pattern from an inner deposit to a thin ring with inner deposit.

## 5 Deposition on a Non-wetted Surface

Regarding the evaporation of droplets on non-wetted (hydrophobic) surfaces, in general, an inner deposit pattern can be found, attributed to the CCA mode of evaporation. On such surfaces, the particles stay inside the evaporating droplet with diminishing contact radius and accumulate at the middle or inner range of the droplet. For example, Nguyen et al.<sup>31</sup> obtained the centralized/inner deposit pattern using a hydrophobic silicon, on which during the evaporation the depinning of contact line occurs bringing the particles to the inner region of the droplet, as shown in Fig. 11. Before that in another study, Orejon et al.<sup>32</sup> studied the droplet evaporation on non-wetted surfaces and showed that the presence of

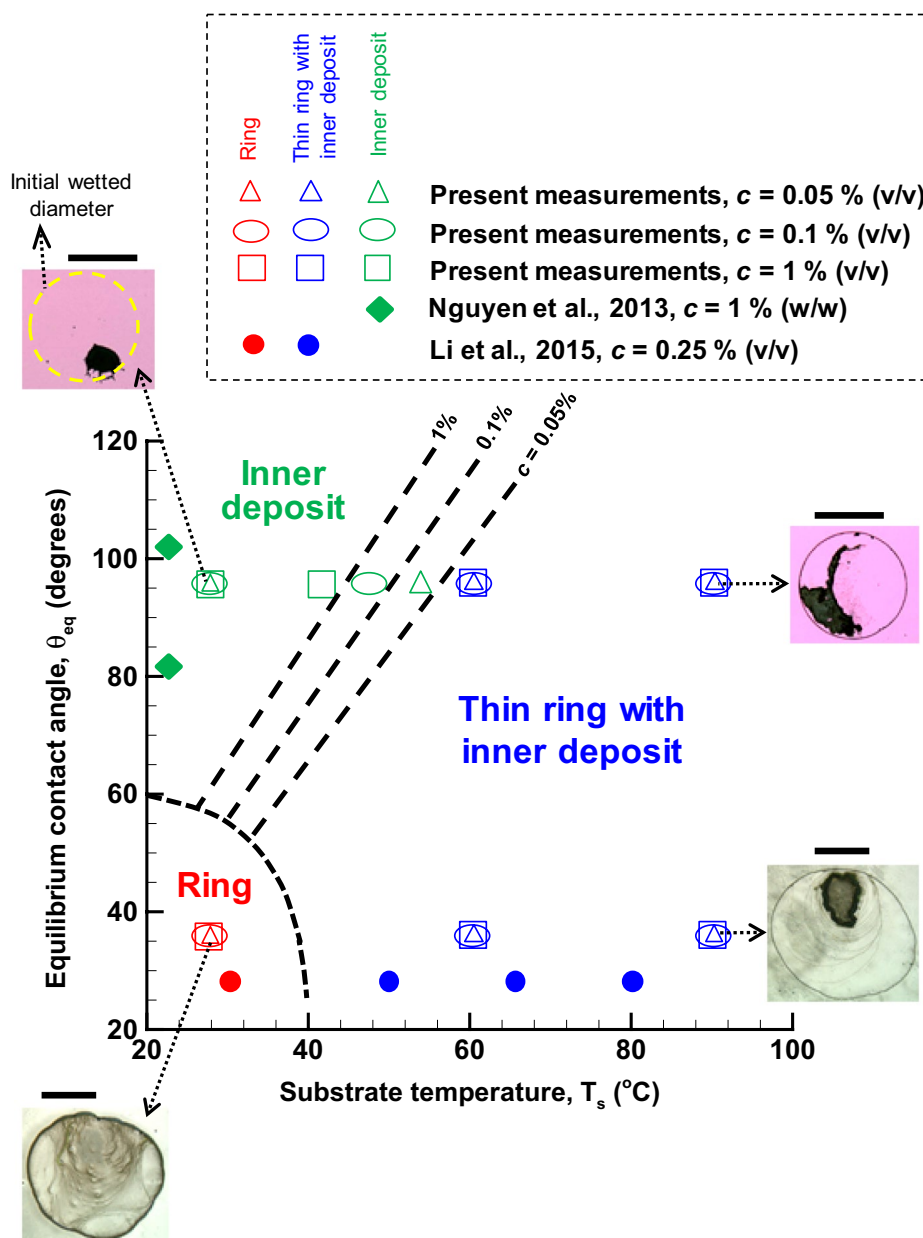


**Figure 8:** Regime map for predicting the deposit patterns as a function of the substrate temperature, substrate wettability and particle concentration. At lower substrate temperature close to ambient, a ring and an inner deposit form on lower and higher contact angle substrates, respectively. At higher substrate temperature, a thin ring with inner deposit forms on all contact angle substrates. Reprinted with permission from Ref. <sup>14</sup>. Copyright (2016) American Chemical Society.

nanoparticles helped in the pinning as well as the stick–slip behavior of the contact line. Larger concentration of particles can delay the depinning of the contact line in comparison to that of the pure liquid droplet. Further, Li et al.<sup>33</sup> studied a controlled deposition of polymer nanoparticles by changing the contact angle hysteresis (CAH). As shown in Fig. 12, the inner deposits formed on

weak CAH (such as poly diallyl-dimethyl ammonium chloride or sodium polysulfonate) and ring-like deposits formed on strong CAH (such as polyvinyl pyrrolidone). Recently, Bhardwaj<sup>34</sup> suggested that the internal motion of the particles inside the droplet on a non-wetted surface is from the contact line to the top of the droplet, due to larger evaporation flux on the top of the droplet, as shown by a schematic in Fig. 13.

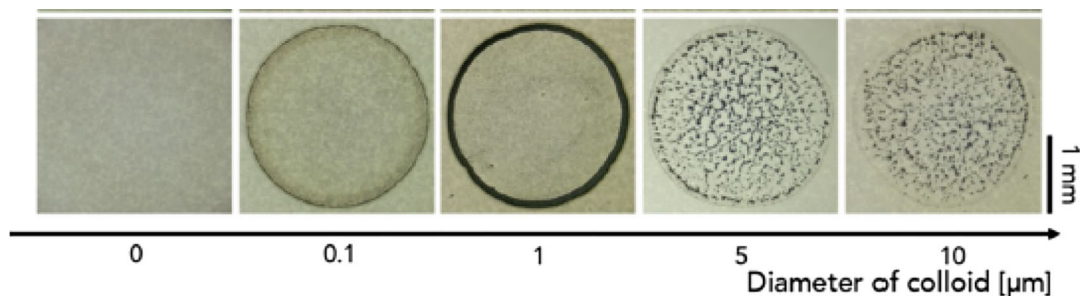


**Figure 9:** Deposit patterns obtained on the glass substrate showing the influence of the particle size inside the evaporating droplet. Reprinted with permission from Ref.<sup>35</sup>. Copyright (2017) Nature Publishing Group.

### 6 Formation of a Uniform Deposit

For application such as ink-jet printing and manufacturing of bioassays, a uniform deposit is required rather than a ring-like or inner deposit. This has been achieved by varying the pH of the suspension in a study by Bhardwaj et al.<sup>35</sup>, using a water–glass–titania system. They proposed a regime diagram for three deposit patterns that can be explained by the competition between three characteristic velocities, namely, the radial velocity ( $V_{rad}$ ) caused by the highest evaporation rate at the contact line, the Marangoni velocity

( $V_{Ma}$ ) due to variation in the surface tension gradient and the velocity ( $V_{DLVO+}$ ) due to attractive electrostatic and van der Waals forces between particles and the substrate (called Derjaguin–Landau–Verwey–Overbeek (DLVO) interactions), as shown in Fig. 14. A ring was formed when  $V_{Ma}$  and  $V_{DLVO+}$  were negligible in comparison to  $V_{rad}$ . A ring with a central bump (i.e., inner deposit) was formed when  $V_{Ma}$  was comparatively higher than  $V_{rad}$  and  $V_{DLVO+}$ , and a uniform deposit was formed when the particle and

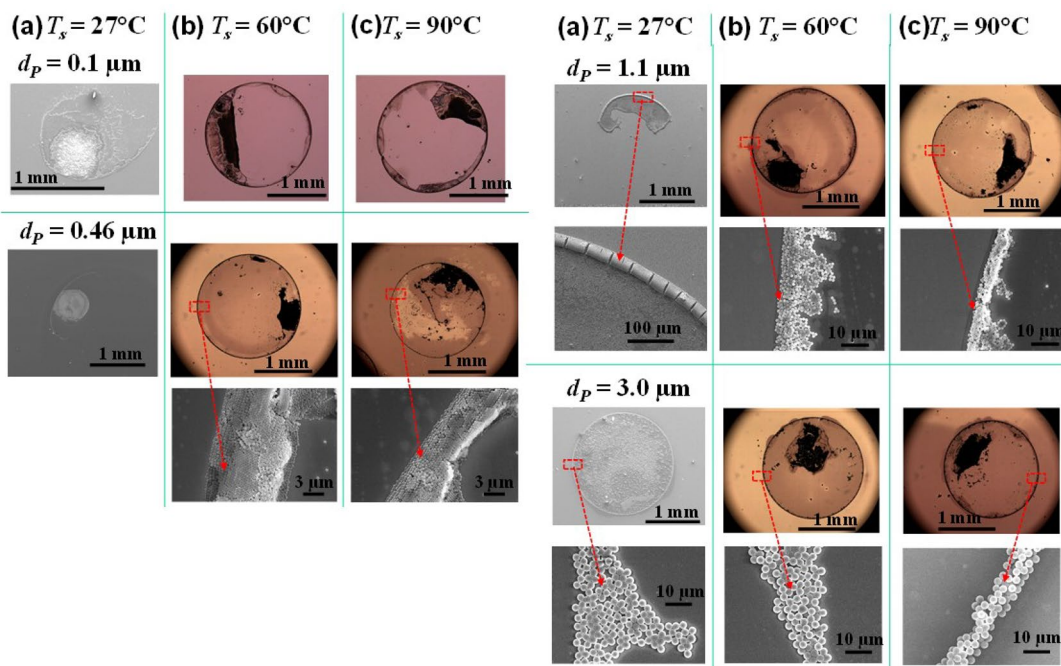


**Figure 10:** Various particle deposit patterns obtained from the combined effect of substrate temperature and particle size on silicon. On non-heated substrate condition, inner deposit forms for smaller size particles and a ring for larger size particles. On heated substrate condition for all particle sizes, a ring with inner deposit forms. The inner deposit corresponds to the Marangoni convection. Reprinted with permission from Ref.<sup>39</sup>. Copyright (2018) American Chemical Society.



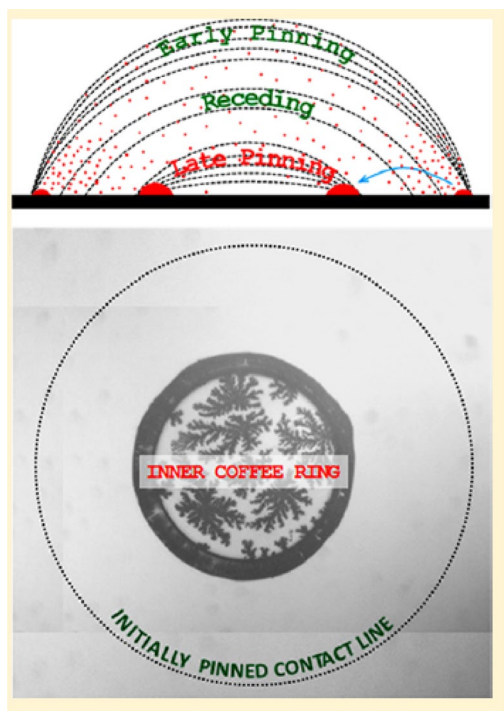


**Figure 11:** Formation of inner deposit on non-wetted surfaces (hydrophobic silicon) due to the contact line receding. Reprinted with permission from Ref.<sup>31</sup>. Copyright (2013) American Chemical Society.

substrate interactions became more dominant than radial and Marangoni velocities.

In another notable report, Still et al.<sup>36</sup> altered the deposition pattern of monodispersed particles ( $1.33 \mu\text{m}$ ,  $c=0.5 \text{ w/w } \%$ ) from the “coffee ring” to a more uniform pattern by adding a surfactant, sodium dodecyl sulfate (SDS). This was explained by the surfactant-induced Marangoni flow. The surfactant was concentrated near the contact line due to the radial flow and higher

evaporation rate closer to the contact line; therefore, the surface tension was decreased locally and induced the Marangoni flow, bringing the particles inward as well as contributing to the depinning of the contact line. Marin et al.<sup>37</sup> investigated the surfactant-driven flow inside a sessile droplet during evaporation on a non-heated glass substrate. Two surfactants, polysorbate 80 (P80) and SDS, were studied. Both radial flow and surface tension difference decreased in the presence of P80 and increased significantly in the presence of SDS. Interestingly, Still et al.<sup>36</sup> and Marin et al.<sup>37</sup> suggested the opposite on the correlation of the surfactant-induced Marangoni flow and the final deposition pattern. Still et al.<sup>36</sup> believed the Marangoni flow can lead to a more uniform deposition, while Marin et al.<sup>37</sup> believed that there was little correlation due to the “rush-hour effect” at the end stage of evaporation.

Uniform deposit patterns can also be obtained by varying particle shape<sup>38, 39</sup>. Yunker et al.<sup>38</sup> studied the evaporation of droplets loaded with ellipsoidal particles and observed uniform deposit patterns. Because of the anisotropic shape of the particles, the interparticle interactions between them generates a loosely packed assembly of particles on the liquid–gas interface and blocks the particles’ advection to the edge; thus, a uniform deposit pattern forms. Dugyala and Basavaraj<sup>39</sup> also reported the controlled uniform deposit pattern formation from the ellipsoidal particles which was achieved due to an attractive particle–particle as well as particle–substrate interactions.

## 7 Particles Sorting in Bi-dispersed Suspensions

As discussed above, the deposits of monodispersed colloidal particle suspension has been studied vastly; however, in recent years utilization of bidispersed colloidal particles has gained

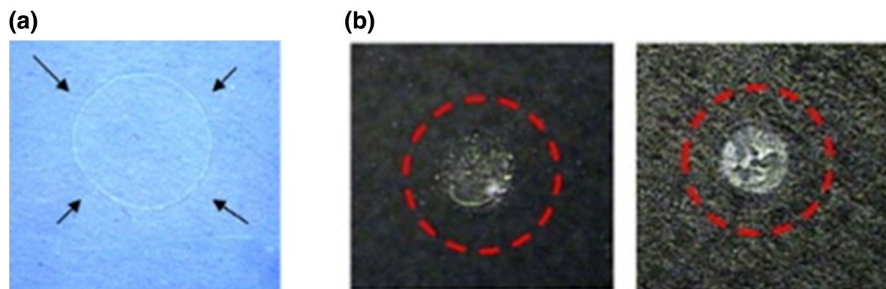


**Figure 12:** Effect of contact angle hysteresis (CAH) in formation of deposit patterns of polymer particles: **a** a ring on high CAH, **b** an inner deposit on weak CAH. Reprinted with permission from Ref.<sup>33</sup>. Copyright (2013) American Chemical Society.

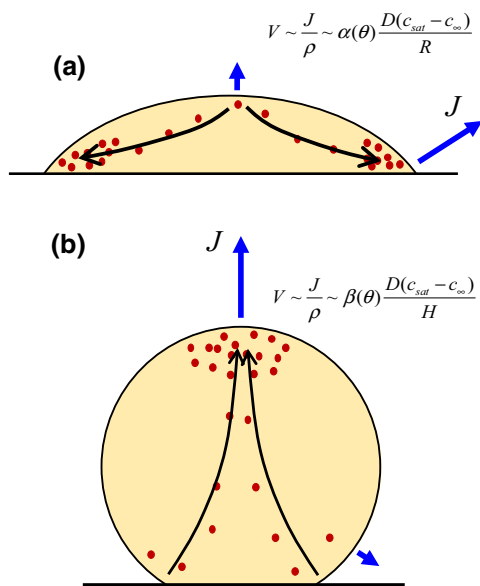


**Figure 13:** Schematic illustration of the advection of colloidal particles (shown as red dots) by evaporation driven flow on partially wetted (a) and non-wetted (b) surface. Blue arrows compare the magnitude of the evaporation flux near the contact and at the apex of the droplet. The respective velocity scaling is also shown. Reprinted with permission from Ref. <sup>34</sup>. Copyright (2018) Elsevier.

attention due to its applications in biochemistry analysis<sup>4</sup>, controlled evaporative self-assembly<sup>40</sup> and biosensors<sup>5</sup>. Specifically, few studies have focused on achieving particle sorting in the deposit. Han et al.<sup>40</sup> observed self-assembly of bidispersed particles (50 nm and 500 nm, 1:1,  $c=0.01\%$  w/w), with smaller particles deposited closer to the contact line and larger ones adjacent to them, in a cylinder-on-flat geometry. The self-sorting feature was attributed to the gradual decrease of the liquid–gas interface height toward the contact line. The particle carried by the radial flow toward the contact line stops when its diameter matches the height of the interface. Therefore, smaller particles can be transported closer to the contact line. Similarly, Chhasatia and Sun<sup>41</sup> investigated the particle sorting by considering the effect of substrate wettability. They used an ink-based bidispersed solution ( $d_p=100$  nm and  $1.1 \mu\text{m}$ ,  $c=0.5\%$  v/v each) on coated glass having different receding contact angles ( $\theta_{\text{rec}}=80, 55, 30, 10,$  and  $0^\circ$ ). They reported that with increase in substrate wettability, a good amount of sorting was seen on substrates having  $0^\circ$  receding contact angle, as shown in Fig. 15. No sorting was seen on substrates having high receding contact angle, as there was formation of an inner deposit.

Further, Monteux and Lequeux<sup>42</sup> studied the effect of particle size combination in bidispersed suspensions. They used three combinations

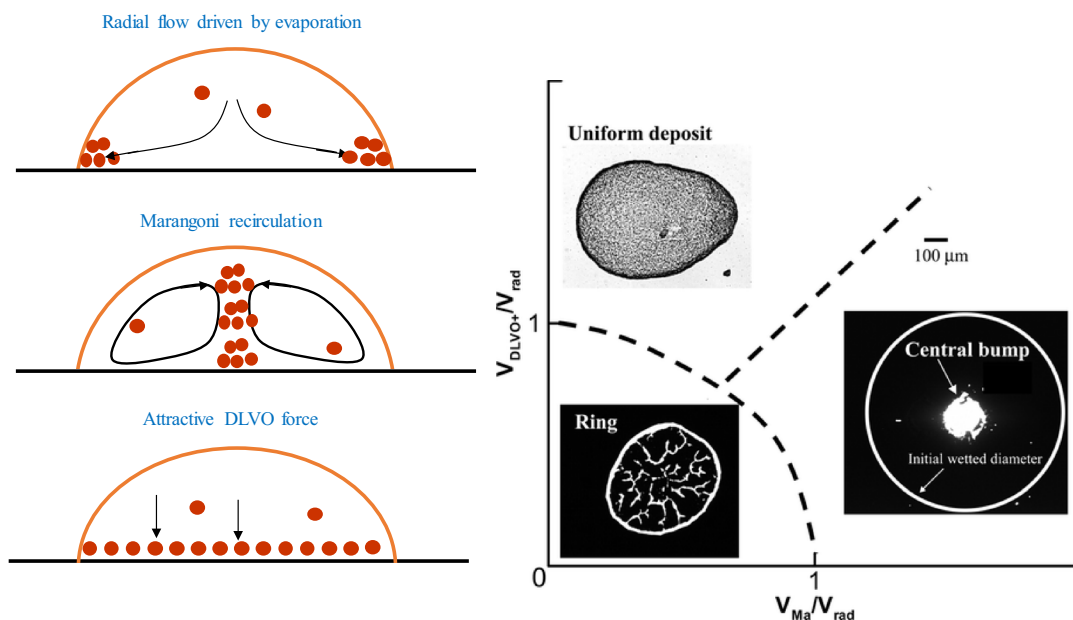


**Figure 14:** Regime map for the deposit patterns considering the effect of pH of the solution and the evaporation mechanism, which involves the competition between three characteristic velocities ( $V_{\text{rad}}$ ,  $V_{\text{Ma}}$  and  $V_{\text{DLVO}}$ ). Reprinted with permission from Ref. <sup>35</sup>. Copyright (2010) American Chemical Society.

( $d_p = 100$  nm and  $1 \mu\text{m}$ ,  $100$  nm and  $5 \mu\text{m}$ ,  $1$  and  $5 \mu\text{m}$ ,  $c = 0.16$ – $1.6\%$  w/w) and observed the particle sorting at the contact line. They observed that at the contact line of the droplet, a thin film region exists depending on the contact angle ( $\theta_{\text{eq}} = 10^\circ$ ) and the particle size. A similar type of thin film region was reported recently by Parsa et al.<sup>43</sup> for bidispersed particles ( $1 \mu\text{m}$  and  $3.2 \mu\text{m}$ ,  $1:1$ ,  $0.025\%$  w/w) on heated silicon. In this study, they reported the effect of substrate temperature ( $T_s = 25$ – $99^\circ\text{C}$ ) during sorting of particles at the contact line. As shown in Fig. 16, a thin film exists at the outermost ring, next to that smaller particles deposited at the middle ring and a mixture of smaller and larger particles deposited at the innermost ring. However, they did not study different particle size combinations. Thereafter, Patil et al.<sup>30</sup> investigated the combined effect of particle size combinations and the substrate temperature on self-sorting of bidispersed colloidal particles on silicon wafer. They proposed a regime map for the observed deposit patterns, as shown in Fig. 17. On non-heated silicon, the depinning of the contact line was seen and, as a result, a mixture of smaller and larger particles was formed. Since heating of a hydrophobic surface induces pinning of the contact line<sup>14</sup>, Patil et al.<sup>30</sup> obtained the sorting of particles in such a system for particle diameter ratio smaller than  $0.18$  and substrate temperature higher than  $60^\circ\text{C}$ . However, in their study, only one substrate was studied. Very recently, Iqbal et al.<sup>44</sup> reported bidispersed colloidal particles on hydrophilic as well as hydrophobic substrates. To devise the particle sorting mechanism, they performed a force analysis on the bidispersed particles near the contact line. Figure 18 shows the schematics of the flow inside the droplet and the obtained final deposit patterns on hydrophilic and hydrophobic substrates. As expected on hydrophilic substrate, sorting of  $0.2$  and  $3 \mu\text{m}$  diameter particles was reported, which was attributed to the dominant radial outward-driven flow and the friction forces

as compared to the inward surface tension force. While on hydrophobic substrate, a mixture of  $0.2$  and  $3 \mu\text{m}$  diameter particles was seen, which was attributed to the dominant inward surface tension-driven forces in comparison to that of other forces.

## 8 Concluding Remarks and Future Outlook

We have reviewed recent key studies, which investigated the formation of a colloidal deposit via the evaporation of a sessile droplet on a solid surface. Several transport phenomena were found to be important in controlling the deposit shape. The radial flow due to the maximum evaporation at the contact line, flow of particles toward the substrate due to electrostatics and van der Waals forces, and Marangoni convection due to thermal gradient at the liquid–gas interface are primary mechanisms in producing a ring-like, uniform and inner deposit, respectively. The Marangoni convection could become intense with the

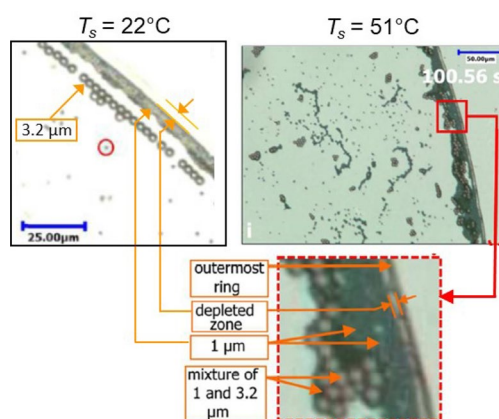


**Figure 16:** Effect of substrate temperature on particle sorting of bidispersed particles from evaporating droplets on silicon. Reprinted with permission from Ref.<sup>43</sup>. Copyright (2017) American Chemical Society.

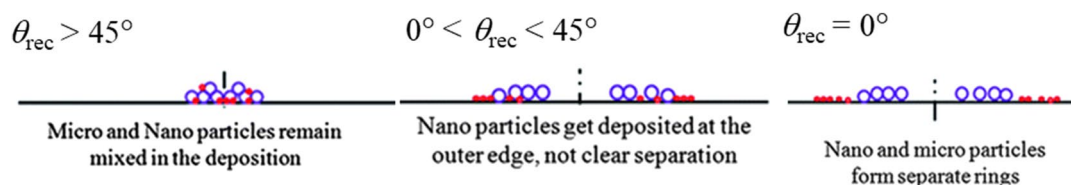


**Figure 15:** Schematic of the particle sorting onto a glass substrate by systematically varying the substrate wettability/contact angle of substrate. Reprinted with permission from Ref.<sup>41</sup>. Copyright (2011) Royal Society of Chemistry.

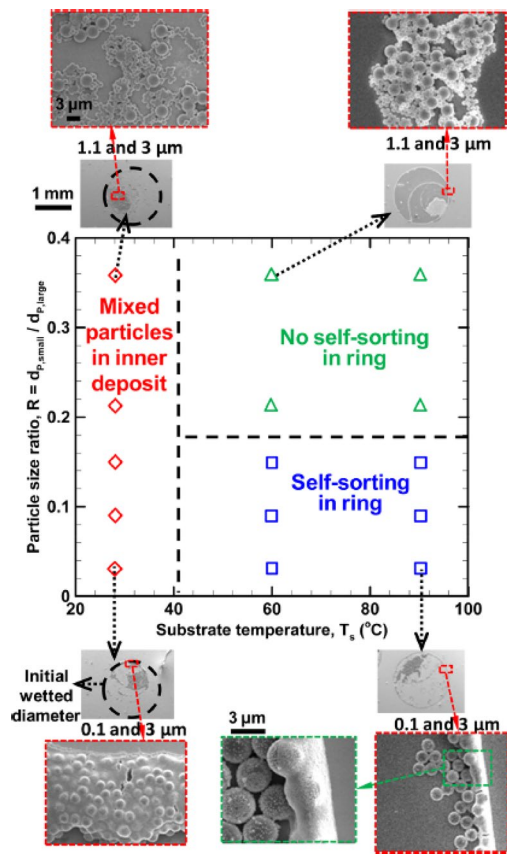


**Figure 17:** Regime map for the bidispersed colloidal particles as a function of the particle size ratio and substrate temperature. Map shows three deposit patterns, namely, mixed particles in inner deposit, self-sorting in ring and no self-sorting in ring. Reprinted with permission from Ref. <sup>30</sup>. Copyright (2018) American Chemical Society.

substrate heating and, coupled with a pinned line, a deposit with a thinner ring and inner deposit forms. The shape of the particles has been reported to be important and a droplet with ellipsoid particles results in a uniform deposit rather than a ring. We discussed the regime maps for different deposit patterns reported in the literature. These maps allow us to classify the deposits and understand the underlying mechanism of the formation of the deposit. We have briefly explained the particles sorting achieved by the evaporation of bidispersed colloidal suspensions on a solid surface. The sorting depends on the ratio of the diameter of the particles and the intensity of substrate heating.

There exist several opportunities for future research in this context. For instance, this knowledge base will help to explain the deposit obtained from the drying of blood droplets which could be useful in forensics<sup>45</sup>, biomarkers<sup>46</sup> and fingerprint residues in blood pattern analysis<sup>6</sup>. In biology, the bio-molecular interaction between the particles and substrate is important to understand the formation of bio-assays<sup>47</sup>. In this review, we tried to consider recent works that studied the effect of substrate heating, particle size and substrate wettability; however, the combined or coupled effect of each of these parameters over another for a wider range is still lacking in the literature. Further, in the last stage of droplet evaporation, the evaporation mechanism is much more complex and transient, since there is a thin film of droplet

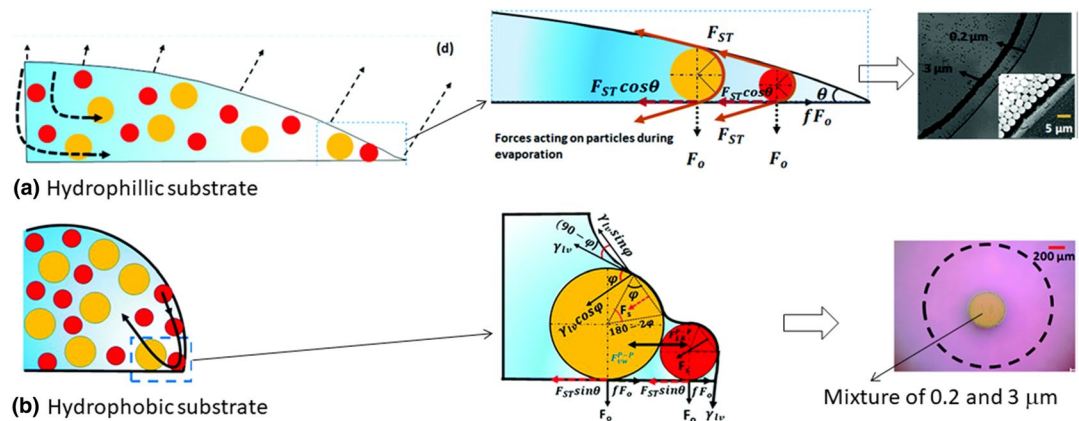


**Figure 18:** Schematics of the fluid flow inside the evaporating droplet containing bidispersed colloidal particles and the forces acting on the particles near the contact line on **a** hydrophillic and **b** hydrophobic substrates. At the contact line, the particle experiences surface tension force ( $F_{ST}$ ), drag force ( $F_D$ ), friction force ( $fF_0$ ), and adhesion forces ( $F_0$ ) due to the van der Waals force and electrostatic interaction forces between particles and substrate as well as among the particles themselves. **a** Sorting of 0.2 and 3  $\mu\text{m}$  diameter particles was seen, which can be attributed to dominant radial outward driven flow and the friction forces. **b** Mixture of 0.2 and 3  $\mu\text{m}$  diameter particles was seen, which can be attributed to the dominant inward surface tension driven forces. Reprinted with permission from Ref. <sup>44</sup>. Copyright (2018) Royal Society of Chemistry.

liquid that evaporates. However, its evaporation mechanism is little explored and it is important to investigate in future, as this last stage of evaporation (known as “rush-hour” effect) could significantly affect the deposit patterns.

### Publisher's Note

Springer Nature remains neutral with regard to jurisdictional claims in published maps and institutional affiliations.

### Acknowledgements

RB gratefully acknowledges financial support by a Grant (EMR/2016/006326) from the Science and Engineering Research Board (SERB), Department of Science and Technology (DST), New Delhi, India.

Received: 5 February 2019 Accepted: 8 February 2019  
Published online: 25 February 2019

### References

- Larson RG (2017) In retrospect: twenty years of drying droplets. *Nature* 550:466
- De Gans BJ, Duineveld PC, Schubert US (2004) Inkjet printing of polymers: state of the art and future developments. *Adv Mater* 16:203–213
- Tekin E, Smith PJ, Schubert US (2008) Inkjet printing as a deposition and patterning tool for polymers and inorganic particles. *Soft Matter* 4:703–713
- Cai Y, Zhang Newby B-M (2008) Marangoni flow-induced self-assembly of hexagonal and stripelike nanoparticle patterns. *J Am Chem Soc* 130:6076–6077
- Wen JT, Ho C-M, Lillehoj PB (2013) Coffee ring aptasensor for rapid protein detection. *Langmuir* 29:8440–8446
- Shiri S, Martin KF, Bird JC (2019) Surface coatings including fingerprint residues can significantly alter the size and shape of bloodstains. *Forensic Sci Int* 295:189–198
- Deegan RD, Bakajin O, Dupont TF, Huber G, Nagel SR, Witten TA (1997) Capillary flow as the cause of ring stains from dried liquid drops. *Nature* 389:827–829
- Bhardwaj R, Longtin JB, Attinger D (2010) Interfacial temperature measurements, high-speed visualization and finite-element simulations of droplet impact and evaporation on a solid surface. *Int J Heat Mass Transf* 53:3733–3744
- Larson RG (2014) Transport and deposition patterns in drying sessile droplets. *AIChE J* 60:1538
- Sefiane K (2014) Patterns from drying drops. *Adv Coll Interface Sci* 206:372–381
- Parsa M, Harmand S, Sefiane K (2018) Mechanisms of pattern formation from dried sessile drops. *Adv Coll Interface Sci* 254:22–47
- Picknett RG, Bexon R (1977) The evaporation of sessile or pendant drops in still air. *J Colloid Interface Sci* 61:336–350
- Sommer AP, Ben-Moshe M, Magdassi S (2004) Self-discriminative self-assembly of nanospheres in evaporating drops. *J Phys Chem B* 108:8–10
- Patil ND, Bange PG, Bhardwaj R, Sharma A (2016) Effects of substrate heating and wettability on evaporation dynamics and deposition patterns for a sessile water droplet containing colloidal particles. *Langmuir* 32:11958–11972
- Maheshwari S, Zhang L, Zhu Y, Chang H-C (2008) Coupling between precipitation and contact-line dynamics: multiring stains and stick-slip motion. *Phys Rev Lett* 100:044503
- Sangani AS, Lu C, Su K, Schwarz JA (2009) Capillary force on particles near a drop edge resting on a substrate and a criterion for contact line pinning. *Phys Rev E* 80:011603
- Jung J-Y, Kim YW, Yoo JY, Koo J, Kang YT (2010) Forces acting on a single particle in an evaporating sessile droplet on a hydrophilic surface. *Anal Chem* 82:784–788
- Wong T-S, Chen T-H, Shen X, Ho C-M (2011) Nano-chromatography driven by the coffee ring effect. *Anal Chem* 83:1871–1873
- Weon BM, Je JH (2013) Self-pinning by colloids confined at a contact line. *Phys Rev Lett* 110:028303
- Li Y, Lv C, Li Z, Quéré D, Zheng Q (2015) From coffee rings to coffee eyes. *Soft matter* 11:4669–4673
- Parsa M, Harmand S, Sefiane K, Biggerelle M, Deltombe R (2015) Effect of substrate temperature on pattern formation of nanoparticles from volatile drops. *Langmuir* 31:3354–3367
- Hu H, Larson RG (2005) Analysis of the effects of Marangoni stresses on the microflow in an evaporating sessile droplet. *Langmuir* 21:3972–3980
- Hu H, Larson RG (2006) Marangoni effect reverses coffee-ring depositions. *J Phys Chem B* 110:7090–7094
- Bhardwaj R, Fang X, Attinger D (2009) Pattern formation during the evaporation of a colloidal nanoliter drop: a numerical and experimental study. *New J Phys* 11:075020
- Zhong X, Duan F (2016) Disk to dual ring deposition transformation in evaporating nanofluid droplets from substrate cooling to heating. *Phys Chem Chem Phys* 18:20664–20671
- Perelaer J, Smith PJ, Hendriks CE, van den Berg AM, Schubert US (2008) The preferential deposition of silica micro-particles at the boundary of inkjet printed droplets. *Soft Matter* 4:1072–1078
- Biswas S, Gawande S, Bromberg V, Sun Y (2010) Effects of particle size and substrate surface properties on deposition dynamics of inkjet-printed colloidal drops for printable photovoltaics fabrication. *J Sol Energy Eng* 132:021010

28. Ryu S-A, Kim JY, Kim SY, Weon BM (2017) Drying-mediated patterns in colloid-polymer suspensions. *Sci Rep* 7:1079
29. Malla LK, Bhardwaj R, Neild A (2019) Analysis of profile and morphology of colloidal deposits obtained from evaporating sessile droplets. *Colloids Surf A Physicochem Eng Asp* 567:150–160
30. Patil ND, Bhardwaj R, Sharma A (2018) Self-Sorting of bidispersed colloidal particles near contact line of an evaporating sessile droplet. *Langmuir* 34:12058–12070
31. Nguyen TA, Hampton MA, Nguyen AV (2013) Evaporation of nanoparticle droplets on smooth hydrophobic surfaces: the inner coffee ring deposits. *J Phys Chem C* 117:4707–4716
32. Orejon D, Sefiane K, Shanahan ME (2011) Stick–slip of evaporating droplets: substrate hydrophobicity and nanoparticle concentration. *Langmuir* 27:12834–12843
33. Li Y-F, Sheng Y-J, Tsao H-K (2013) Evaporation stains: suppressing the coffee-ring effect by contact angle hysteresis. *Langmuir* 29:7802–7811
34. Bhardwaj R (2018) Analysis of an evaporating sessile droplet on a non-wetted surface. *Colloid Interface Sci Commun* 24:49–53
35. Bhardwaj R, Fang X, Somasundaran P, Attinger D (2010) Self-assembly of colloidal particles from evaporating droplets: role of DLVO interactions and proposition of a phase diagram. *Langmuir* 26:7833–7842
36. Still T, Yunker PJ, Yodh AG (2012) Surfactant-induced Marangoni eddies alter the coffee-rings of evaporating colloidal drops. *Langmuir* 28:4984–4988
37. Marin A, Liepelt R, Rossi M, Kähler CJ (2016) Surfactant-driven flow transitions in evaporating droplets. *Soft Matter* 12:1593–1600
38. Yunker PJ, Still T, Lohr MA, Yodh A (2011) Suppression of the coffee-ring effect by shape-dependent capillary interactions. *Nature* 476:308–311
39. Dugyala VR, Basavaraj MG (2014) Control over coffee-ring formation in evaporating liquid drops containing ellipsoids. *Langmuir* 30:8680–8686
40. Han W, Byun M, Lin Z (2011) Assembling and positioning latex nanoparticles via controlled evaporative self-assembly. *J Mater Chem* 21:16968–16972
41. Chhasatia VH, Sun Y (2011) Interaction of bi-dispersed particles with contact line in an evaporating colloidal drop. *Soft Matter* 7:10135–10143
42. Monteux CC, Lequeux FO (2011) Packing and sorting colloids at the contact line of a drying drop. *Langmuir* 27:2917–2922
43. Parsa M, Harmand S, Sefiane K, Biggerelle M, Deltombe R (2017) Effect of substrate temperature on pattern formation of bidispersed particles from volatile drops. *J Phys Chem B* 121:11002–11017
44. Iqbal R, Majhy B, Shen AQ, Sen A (2018) Evaporation and morphological patterns of bi-dispersed colloidal droplets on hydrophilic and hydrophobic surfaces. *Soft Matter* 14:9901–9909
45. Attinger D, Moore C, Donaldson A, Jafari A, Stone HA (2013) Fluid dynamics topics in bloodstain pattern analysis: comparative review and research opportunities. *Forensic Sci Int* 231:375–396
46. Brutin D, Sobac B, Loquet B, Sampol J (2011) Pattern formation in drying drops of blood. *J Fluid Mech* 667:85–95
47. Hurth C, Bhardwaj R, Andalib S, Frankiewicz C, Dobos A, Attinger D et al (2015) Biomolecular interactions control the shape of stains from drying droplets of complex fluids. *Chem Eng Sci* 137:398–403



**Dr. Nagesh D. Patil** is currently a postdoctoral researcher in the Mechanical Engineering Department at University of British Columbia, Vancouver, Canada. Prior to that, he received his Ph.D. from I.I.T. Bombay in 2018 and M.S. from I.I.T. Kharagpur in 2011. His research interest includes droplet impact and evaporation dynamics, colloidal particles deposit patterns, multiphase flows, textured surfaces, computational fluid dynamics, microfluidics, and thermo-hydraulics for nuclear reactor. He has hands-on experience of several experimental techniques such as high-speed visualization, infrared thermography, confocal microscopy, surface profilometry, scanning electron microscopy (SEM), and image processing. He also has experience in contact line modeling simulations for droplet impact problem using in-house code based on a

dual-grid-level-set-method developed at I.I.T. Bombay. Currently, he is working on particle sorting in an evaporating droplet containing bi-dispersed colloidal particles.



**Dr. Rajneesh Bhardwaj** is currently serving as Associate Professor in the Mechanical Engineering Department at I.I.T. Bombay, Mumbai, India. His research interests are in droplets, interfacial flows, and fluid–structure interaction. He earned his Ph.D. with distinction from Columbia University, New York, USA, in 2009 and was a postdoctoral fellow at Johns Hopkins University, Baltimore, USA, before joining I.I.T in 2012. He is a member of The National Academy of Sciences (NASI) and won Young Engineer Award from Indian National Academy of Engineering (INAE) in 2014.